

Handling and Mechanical Properties of Low-viscosity Bulk-fill Resin Composites

E Hirokane • T Takamizawa • T Tamura • S Shibasaki
A Tsujimoto • WW Barkmeier • MA Latta • M Miyazaki

Clinical Relevance

Some low-viscosity bulk-fill resin composites can probably be used in stress-bearing areas, while maintaining an effective depth of cure and good handling properties.

SUMMARY

This study aimed to evaluate the filler contents (FCs), flexural properties, depth of cure (DOC), wear resistance, and handling properties of different low-viscosity bulk-fill resin composites (LVBRCs) and to determine the correlations between the tested parameters. Six LVBRCs, Beautifil-Bulk (BBF), Bulk Base Hard (BBH), Bulk Base Medium (BBM), Filtek Bulk-Fill Flowable Restorative (FBF), G-aenial Bulk Injectable (GBI), and SDR flow+ Bulk-Fill Flowable (SDR) were used. The DOC and flexural property tests were conducted according to the ISO 4049 specifications. The flexural

strength, elastic modulus, and resilience were determined in 12 specimens that were obtained from each of the 6 materials. Sliding-impact-wear testing was conducted by evaluating the wear facets of the specimens using a noncontact profilometer and by confocal laser scanning microscopy. The handling properties of the LVBRC was assessed *via* extrusion force and thread formation measurements. The DOC for the majority of the LVBRCs was approximately 4 mm. Although the FCs and mechanical properties were material dependent, some LVBRCs exhibited excellent flexural properties and wear resistance. The LVBRCs demonstrated a wide range of extrusion force and thread formation. Regarding the correlations

Eizo Hirokane, DDS, Department of Operative Dentistry, Nihon University Graduate School of Dentistry, Tokyo, Japan

*Toshiki Takamizawa, DDS, PhD, Department of Operative Dentistry, Nihon University School of Dentistry, Tokyo, Japan

Tomohiko Tamura, DDS, Department of Operative Dentistry, Nihon University Graduate School of Dentistry, Tokyo, Japan

Sho Shibasaki, DDS, PhD, Department of Operative Dentistry, Nihon University School of Dentistry, Tokyo, Japan

Akimasa Tsujimoto, DDS, PhD, Department of Operative Dentistry, University of Iowa College of Dentistry, Iowa City, IA, USA

Wayne W. Barkmeier, DDS, MS, Department of General Dentistry, Creighton University School of Dentistry, Omaha, NE, USA

Mark A. Latta, DMD, MS, Department of General Dentistry, Creighton University School of Dentistry, Omaha, NE, USA

Masashi Miyazaki, DDS, PhD, Department of Operative Dentistry, Nihon University School of Dentistry, Tokyo, Japan

*Corresponding author: 1-8-13, Kanda-Surugadai, Chiyoda-ku, Tokyo, Japan; e-mail: Takamizawa.toshiki@nihon-u.ac.jp

<https://doi.org/10.2341/20-253-L>

between the tested parameters, extremely strong negative and positive correlations were observed for the DOC versus extrusion force, flexural strength versus elastic modulus, maximum depth versus volume loss, and maximum depth versus thread formation. In addition, strong correlations between FCs and DOC, resilience, wear resistance, and extrusion force were observed.

INTRODUCTION

Over the decades, technological innovations have been mitigating the drawbacks of resin composites, such as the mechanical properties, polymerization shrinkage, color match, polishability, depth of cure (DOC), and handling properties.¹ In particular, the development of low-viscosity resin composites, namely, flowable resin composites, had a huge impact on restorative dentistry owing to their ease of handling.² Flowable resin composites possess high flowability and low viscosity; therefore, they can be used to restore any kind of cavity with small-gage dispensers and as a liner on the cavity floor to reduce the development of air bubbles.³ Various improvements in flowable resin composites have been made since their introduction into the market in the early 1990s. Currently, these materials have a much broader range of applicability, and various types of flowable resin composites with different viscosities and flowabilities suitable for a variety of cavity conditions are available.⁴⁻⁶

The mechanical properties of some of the recent flowable resin composites are equal or superior to those of conventional resin composites; hence, they can be used for high-stress-bearing areas, large cavities, and class II restorations.^{2,5} In our previous study, we compared the wear resistance between recent flowable and conventional resin composites, and found that four out of the six tested flowable resin composites did not exhibit any significant differences in maximum wear depth and volume loss, after slinging-impact wear testing, when compared with a nanofiller resin composite. However, the wear resistance of these materials was significantly higher than that of a hybrid-type conventional resin composite.² In addition to the superior mechanical properties and wear resistance, “injectable” flowable resin composites have good handling properties when used to create anatomical features, marginal ridges, and molar cusps.

Bulk-fill resin composites (BRCs) were developed to reduce the contraction stress and the number of filling steps.⁷⁻⁹ They can be used as a single layer (up

to 4 mm in thickness) with adequate C=C double bond conversion and short activation times owing to their increased translucency properties and the presence of modified photoinitiators and resin monomers.¹⁰⁻¹³ This new type of resin composite is promising for use not only in deep cavities but also as a direct core foundation material. BRCs can be classified into two types: low-viscosity type similar to flowable resin composites and high-viscosity type resembling conventional resin composites.¹⁴ Moreover, they can be classified based on the mode of use as base composites or final filling restoratives, which do not need an additional resin paste.^{8,14}

Low-viscosity BRCs (LVBRCs) are used more frequently for base materials, owing to their inferior mechanical properties and their ability to conform to the cavity floor more easily, as compared with high-viscosity materials.^{8,14,15} However, some LVBRCs are thought to have mechanical properties similar to those of high-viscosity BRCs, along with good handling properties, due to recent advances in flowable resin composite technology.¹⁶ Therefore, it is likely that LVBRCs will be used as final filling restoratives, as for high-viscosity BRCs or flowable resin composites with advanced properties. However, information on the mechanical properties, wear resistance, or handling properties of LVBRCs is scarce.

The purpose of this study was to investigate some of the mechanical properties of LVBRCs, including the filler content, DOC, flexural properties, wear resistance, and handling properties. The null hypotheses to be tested were as follows: (1) the mechanical properties, wear, and handling properties of the tested LVBRCs would not be affected by the type of LVBRC used, (2) no correlations between the tested parameters would be observed.

METHODS AND MATERIALS

Study Materials

The six LVBRCs used in this study were as follows (Table 1): Beautifil-Bulk (BBF; Shofu, Kyoto, Japan), Bulk Base Hard (BBH, Sun Medical, Shiga, Japan), Bulk Base Medium (BBM, Sun Medical), Filtek Bulk-Fill Flowable Restorative (FBF, 3M Oral Care, St. Paul, MN, USA), G-aenial Bulk Injectable (GBI, GC, Tokyo, Japan), and SDR flow+ Bulk-Fill Flowable (SDR, Dentsply Sirona, Charlotte, NC, USA).

A halogen-quartz-tungsten curing unit (Optilux 501; SDS Kerr, Danbury, CT, USA) was used,¹⁷ and the light irradiance (600 mW/cm²) of the curing unit

Table 1: *Materials Used in This Study*^a

Code	Resin Composite (Shade; Lot No.)	Main Components	Manufacturer
Low-viscosity bulk-fill resin composite			
BBF	Beautifil Bulk Flowable (Universal; 071934)	<i>bis</i> -GMA, UDMA, <i>bis</i> -MPEPP, TEGDMA, fluoroaluminosilicate glass, reaction initiator, others	Shofu, Kyoto, Japan
BBH	Bulk Base Hard (Universal; TK12)	<i>bis</i> -MPEPP, urethane acrylate, barium glass filler, strontium aluminosilicate glass, initiator, aromatic amine, others	Sun Medical, Shiga, Japan
BBM	Bulk Base Medium Flow (Universal; TL12)	<i>bis</i> -MPEPP, urethane acrylate, barium glass filler, strontium aluminosilicate glass, aromatic amine	Sun Medical, Shiga, Japan
FBF	Filtek Bulk Fill Flowable restorative (Universal; NA10949)	<i>bis</i> -GMA, UDMA, <i>bis</i> -EMA, procrylat resins, TEGDMA, zirconia/silica filler, ytterbium trifluoride filler	3M Oral Care, St. Paul, MN, USA
GBI	G-aenial Bulk Injectable (Universal; 1906292)	<i>bis</i> -EMA, dimethacrylate, bismethacrylate, dimethacrylate component, UDMA, UV-light absorber, silane, silica, barium glass filler, photoinitiator, stabilizers, pigments	GC, Tokyo, Japan
SDR	SDR flow+ Bulk Fill Flowable (Universal; 17339)	modified urethane dimethacrylate resin, TEGDMA, polymerizable dimethacrylate resin, BHT, polymerizable trimethacrylate resin, ethyl-4(dimethylamino)benzoate photoaccelerator silanated barium-alumino-fluoroborosilicate glass silanated strontium aluminofluorosilicate glass, surface treated fume silicas, ytterbium fluoride, pigments	Dentsply Sirona, Charlotte, NC, USA

^a Light irradiation time was followed manufacturer's instructions (20 seconds) for a halogen curing light unit.
Abbreviations: *bis*-GMA, 2, 2-bis[4-(2-hydroxy-3-methacryloyloxypropoxy)phenyl] propane; UDMA, urethane dimethacrylate; *bis*-MPEPP, 2, 2'-bis(4-methacryloxy polyethoxyphenyl) propane; TEGDMA, triethylene glycol dimethacrylate; *bis*-EMA, bisphenol A ethoxylate dimethacrylate; BHT, butylated hydroxy toluene.

was checked using a dental radiometer (Model 100, Kerr). In order to standardize light irradiation conditions for each test and material, the guide tip of the curing unit was attached on the transparent matrix tape directly, and irradiation was performed for 20 seconds. Light irradiation time was followed as per the manufacturer's instructions.

Inorganic Filler Content (FC)

The inorganic filler contents (FCs) of the tested LVBRCs were measured using a dental laboratory furnace. Approximately 50 mg of resin paste from each LVBRC was placed in a crucible, a cylindroid of pure platinum that was 7 mm in diameter and 10 mm in depth, and heated in the electric furnace from 25°C to 700°C until the organic components were completely incinerated. The weight of the residual resin paste was measured using an electronic balance (AE163; Mettler-Toledo, Greifensee, Zürich, Switzerland) with an accuracy of ± 0.1 mg, and the FC (wt%) was calculated. Five measurements were obtained for each resin, and the average FC (wt%) was determined.

Depth of Cure (DOC)

Measurements of the depth of cure (DOC) for the LVBRCs were conducted in a 4-mm-diameter and 10-mm-high plastic cylinder in accordance with the

international standard, ISO 4049.¹⁸ The mold was placed on a glass slide covered with a matrix tape (Matrix Tape and Dispenser; 3M Oral Care). Then, it was filled in bulk with one of the tested composites. The topside of the mold was covered with a transparent matrix tape, and the resin paste was pressed flush with the mold using a second glass slide. Ten specimens were irradiated from the top of the cylinder mold with 600 mW/cm² light irradiance for 20 seconds. As soon as the curing was over, the material was pressed out of the mold, and the unpolymerized part was removed using a plastic spatula and cotton dipped in alcohol. The remaining cured part was measured using a digital caliper (CPM15-25DM; Mitutoyo, Tokyo, Japan) with an accuracy of ± 0.1 mm, and the measured value was divided by two, as specified by ISO 4049. This value was recorded as the DOC for each specimen.

Flexural Strength Test

The flexural properties of the LVBRCs were tested according to ISO 4049.¹⁸ A stainless steel split mold (dimensions 25×2×2 mm) was set on a glass slide covered with a matrix strip. Each resin composite paste was filled into the mold, and the topside of the mold was covered with a transparent matrix tape. The resin paste was pressed with a second glass slide under a 5 N load. The middle-third of the specimen

was irradiated for 20 seconds, followed by the remaining thirds for 20 seconds each. The opposite side was irradiated in the same manner. After removing the hardened specimen from the mold, all the six sides were wet polished with #1200-grit SiC paper (Fuji Star Type DDC; Sankyo Rikagaku, Saitama, Japan). Baseline specimens were stored in distilled water at 37°C under dark conditions for 24 hours before the flexural strength test was conducted. The other prepared specimens were similarly stored in distilled water at 37°C for 24 hours under dark conditions before being subjected to 30,000 thermal cycles (TC) between 5°C and 55°C, with a dwell time of 30 seconds.

After the storage period, 12 specimens per test group were subjected to the three-point bending test using a universal testing machine (model 5500R; Instron, Canton, MA, USA) at a crosshead speed of 1.0 mm/minute until the breaking of the specimen. The specimens were set on the three-point bending apparatus with a span length of 20.0 mm. The flexural strength (σ_F) in MPa was calculated as follows:

$$\sigma_F = 3P \bullet D / 2W \bullet H^2,$$

where P =peak load, D =distance between the supports (20 mm), W =width, and H =height.

The elastic modulus (E) in GPa was determined from the stress-strain curve using a computer software program (Bluehill version 2.5; Instron) linked to the testing device. The modulus of resilience (R) was calculated using the following equation¹⁹:

$$R = \sigma_F^2 / 2E$$

Sliding-Impact Simulated Wear Test

The wear properties of the 12 specimens from each group were determined using a sliding-impact-wear testing machine (K655-06; Tokyo Giken, Tokyo, Japan). A polytetrafluoroethylene cylindrical mold (6 mm in diameter and 2 mm in height) was set on a glass slide covered with a matrix strip. Each LVBRC paste was condensed into the mold, and the top side was covered with a transparent matrix tape. The resin paste was pressed through a glass slide under a 5 N load and light irradiated for 20 seconds. One flat surface of each specimen was polished using a sequence of SiC papers up to 2000 grit. Subsequently, they were stored under dark conditions in distilled water at 37°C for 24 hours.

The specimens were attached to the center of a custom fixture made of cold-cured acrylic resin (Tray Resin II, Shofu, Kyoto, Japan) with a small amount of repair glue before wear testing. A stainless steel ball bearing (radius 2.4 mm) set inside a collet assembly was used as an antagonist for the wear-simulation test. The simulator contained a plastic water bath with a constant provision of distilled water at 37°C. Four custom fixtures were positioned inside the bath. During the wear-simulation test, the antagonists directly impacted the specimens from above with a maximum force of 50 N at a rate of 0.5 Hz and slid horizontally for 2 mm. Each specimen was subjected to 50,000 cycles of the sliding-impact motion.

Sliding-Impact Wear Measurements

After the wear-simulation test, the specimens were ultrasonically cleaned with distilled water for 1 minute. The wear facets were evaluated using a confocal laser scanning microscope (CLSM, VK-9710; Keyence, Osaka, Japan) and its built-in software (VK-Analyzer, Keyence). The maximum facet depth (MD in μm) and volume loss (VL in mm^3) of each wear facet were measured.

Extrusion Force Measurement

The extrusion force and thread formation (stickiness) were determined, as described previously.² A universal testing machine (model 5500R; Instron) was used to determine the extrusion force of the tested materials. A special jig was prepared to fix a syringe containing unused fresh LVBRC at the flange, and the plunger was subjected to perpendicular load stress at a crosshead speed of 10 mm/minute. The load stress was automatically monitored during the test, which ended when the resin paste was completely discharged from the syringe. The extrusion force of the resin composite was measured by the peak load stress (MPa) over the course of the testing. Six measurements were performed for each LVBRC.

Thread Formation Property (Stickiness)

A creepmeter (Rheoner II, model RE 2-3305C; Yamaden, Tokyo, Japan) was used to measure the thread formation of the tested LVBRCs. The test resin pastes were filled into a cylindrical mold (diameter, 10 mm; height, 2 mm) made of polytetrafluoroethylene and left for 3 minutes to relieve the internal stresses. A cylindrical rod (diameter 5 mm) was inserted up to 1 mm into the resin paste and pulled up at a crosshead speed of 10 mm/second.

Thread formation was continuously monitored using a video camera (HDR-CX680; Sony, Tokyo, Japan). The vertical distance from the bottom of the rod to the top of the mold (mm) was measured at the point at which the thread broke. Six measurements were performed for each LVBRC.

Scanning Electron Microscope (SEM) Observations

Each cured specimen was polished with abrasive disks (Fuji Star Type DDC), followed by a series of diamond pastes down to a particle size of 0.25 μm (DP-Paste; Struers, Ballerup, Denmark). The polished surfaces were subjected to argon ion beam etching (IIS-200ER, Elionix, Tokyo, Japan) for 45 seconds, with the ion beam directed perpendicular to the polished surface (accelerating voltage, 1 kV; ion current density, 0.4 mA/cm²). The surfaces were then coated with a thin film of gold in a Quick Coater vacuum evaporator (Type SC-701; Sanyu Denchi, Tokyo, Japan). Observations were conducted via scanning electron microscopy (SEM; FE-8000; Elionix) at an operating voltage of 10 kV and under magnifications of 5000 \times and 20000 \times .

SEM examinations were conducted at the center of the wear facets on the tested LVBRCs. The specimens were randomly selected after the wear measurements; the coating of samples was performed as described for the polished specimens. The coated surfaces were visualized using SEM with an operating voltage of 10 kV (magnification 2500 \times).

Statistical Analysis

To determine the appropriate sample size for each test, a statistical power analysis was conducted. The tests were initially performed with sample sizes of 5 for inorganic filler content measurement; 12 for flexural strength, DOC tests, and simulated wear measurements; and 6 for extrusion force and thread formation measurements. After gathering the data, post hoc power tests were conducted using two statistical software systems (G Power calculator and SigmaPlot version 13.0, Systat Software, Chicago, IL, USA) with an f value of 0.75, α value of 0.05, and power of 0.95. The tests indicated that the sample size for each test was adequate.

Owing to the homogeneity of variance (Bartlett test) and normal distribution (Kolmogorov–Smirnov test), the data for each material were subjected to the one-way analysis of variance test followed by Tukey honest significant difference test at a significance level of 0.05. The Pearson product-moment

Table 2: Inorganic Filler Contents (FCs) and Depth of Cure (DOC) of the LVBRCs^a

	Inorganic Filler Content wt%	DOC mm
BBF	69.4 (0.6) a	3.87 (0.06) c
BBH	69.6 (0.7) a	3.10 (0.05) d
BBM	69.5 (0.3) a	3.18 (0.13) d
FBF	61.4 (0.6) c	4.36 (0.06) a
GBI	67.7 (0.5) b	3.93 (0.03) c
SDR	69.0 (0.4) a	4.13 (0.12) b

^a Values in parentheses indicate standard deviation.
Same lowercase letter indicates no difference at 5% significance level.

correlation coefficient was employed for pairwise comparisons to evaluate the interrelationships between the tested parameters. All statistical analyses were conducted using a software system (Sigma Plot).

RESULTS

Inorganic Filler Content

The average inorganic FC in the tested LVBRCs ranged from 61.4 to 69.6 wt% (Table 2). The tested materials listed in descending order of the inorganic filler content were BBH, BBM, BBF, SDR, GBI, and FBF. FBF exhibited a significantly lower inorganic filler content than the other bulk-fill composites.

Depth of Cure

The results of the DOCs are presented in Table 2. The average values in the tested LVBRCs ranged from 3.10 to 4.36 mm. The tested materials listed in descending order based on the DOCs were FBF, SDR, GBI, BBF, BBM, and BBH. FBF exhibited a significantly higher DOC than the other BRC. No significant difference in DOC was observed between BBH and BBM; however, the values of these two materials were significantly lower than those of the remaining four materials (Table 2).

Flexural Properties

The flexural strengths (σ_F) of the LVBRCs are presented in Table 3. At baseline (24-hours water storage group), the mean σ_F values of the LVBRCs ranged from 102.0 to 143.9 MPa. BBH and GBI exhibited significantly higher σ_F values than the other LVBRCs. BBM presented with the lowest σ_F value ($p < 0.05$) among the materials tested. In the TC group, the mean σ_F value of the LVBRCs ranged from 93.1 to 134.0 MPa, and the changing rates were -4.8% to -14.3% , when the σ_F value of baseline is defined as 100%. BBH and GBI exhibited signifi-

Table 3: Influence of Thermal Cycling on Flexural Strength of the LVBRCs ^a			
	Baseline MPa	TC 30,000 MPa	Changes %
BBF	122.5 (6.9) bA	105.0 (7.5) bcB	−14.3
BBH	140.7 (6.1) aA	134.0 (5.6) aB	−4.8
BBM	102.0 (6.9) cA	93.1 (4.5) dB	−8.9
FBF	117.4 (8.5) bA	103.0 (4.9) cB	−12.3
GBI	143.9 (7.1) aA	129.4 (6.6) aB	−10.0
SDR	122.0 (6.8) bA	111.0 (5.5) bB	−9.1
^a Values in parentheses indicate standard deviation. Same lowercase letter in vertical columns indicates no difference at 5% significance level. Same uppercase letter in horizontal rows indicates no difference at 5% significance level.			

cantly higher σ_F values than the other LVBRCs ($p<0.05$), whereas BBM had the lowest σ_F value when compared with the other LVBRCs. A statistically significant reduction in σ_F after TC was observed in each material, when compared with the baseline values.

The elastic moduli (E) of the LVBRCs are presented in Table 4. The mean value of E ranged from 4.1 to 8.4 GPa in the baseline group. BBH and BBM presented with significantly higher and lower E values, respectively, than the other LVBRCs. In the TC group, the mean E values of LVBRCs ranged from 4.4 to 9.5 GPa, and the changing rates were +6.0% to +18.1%. Although no significant difference was observed among BBF, BBH, and GBI, they presented with significantly higher E values than the other LVBRCs. In most of the cases, the E values of the LVBRCs were significantly higher in the TC group than in the baseline group.

The resilience (R) values of the BRCs are presented in Table 5. The mean R in the baseline group ranged from 1.0 to 1.3 MJ/mm³. BBF exhibited a

Table 4: Influence of Thermal Cycling on Elastic Modulus of the LVBRCs ^a			
	Baseline GPa	TC 30,000 GPa	Changes %
BBF	7.2 (0.3) bA	8.5 (1.3) aB	+18.1
BBH	8.4 (0.4) aA	8.9 (0.7) aA	+6.0
BBM	4.1 (0.2) eA	4.4 (0.3) cB	+7.3
FBF	5.5 (0.4) dA	6.3 (0.3) bB	+14.5
GBI	7.7 (0.6) bA	8.8 (1.2) aB	+14.3
SDR	6.4 (0.7) cA	7.0 (0.5) bB	+9.3
^a Values in parentheses indicate standard deviation. Same lowercase letter in vertical columns indicates no difference at 5% significance level. Same uppercase letter in horizontal rows indicates no difference at 5% significance level.			

Table 5: Influence of Thermal Cycling on Resilience of the LVBRCs ^a			
	Baseline MJ/mm ³	TC 30,000 MJ/mm ³	Changes %
BBF	1.0 (0.1) bA	0.6 (0.1) cB	−40.0
BBH	1.2 (0.1) aA	1.0 (0.1) aB	−17.7
BBM	1.2 (0.2) aA	1.0 (0.1) aB	−17.7
FBF	1.3 (0.1) aA	0.8 (0.1) bB	−38.5
GBI	1.3 (0.1) aA	1.0 (0.2) aB	−23.1
SDR	1.2 (0.1) aA	0.9 (0.1) aB	−25.0
^a Values in parentheses indicate standard deviation. Same lowercase letter in vertical columns indicates no difference at 5% significance level. Same uppercase letter in horizontal rows indicates no difference at 5% significance level.			

significantly lower R than the other LVBRCs. For all the materials, statistically significant reductions in R were observed after TC when compared with the baseline, and the changing rates were −17.7% to −40%.

Sliding-Impact Simulated Wear Test

The MD and VL of the LVBRCs after the sliding-impact-wear test are presented in Table 6. The mean value of the MD and VL ranged from 44.0 to 208.6 μm and from 0.022 and 0.443 mm³, respectively. The LVBRCs were classified into high- and low-wear resistance groups based on the wear behavior. BBH, FBF, and GBI exhibited a significantly higher wear resistance than BBF, BBM, and SDR.

Handling Properties

The flowability (extrusion force and thread formation) relating to the handling of the LVBRCs are presented in Table 7. The mean extrusion force value ranged from 0.10 to 0.37 MPa. SDR demonstrated a significantly lower extrusion force than the other LVBRCs; conversely, BBH and BBM exhibited

Table 6: Maximum Facet Depth (MD) and Volume Loss (VL) after Sliding-impact Wear Test ^a		
	MD μm	VL mm ³
BBF	174.5 (32.1) a	0.414 (0.08) a
BBH	49.2 (6.5) b	0.025 (0.0002) b
BBM	208.6 (33.4) a	0.443 (0.07) a
FBF	51.2 (6.9) b	0.034 (0.004) b
GBI	44.0 (9.7) b	0.022 (0.006) b
SDR	208.1 (47.9) a	0.390 (0.09) a
^a Values in parentheses indicate standard deviation. Same lowercase letter in vertical columns indicates no difference at 5% significance level.		

Table 7: Handling Properties of the LVBRCs^a

	Extrusion force MPa	Thread formation mm
BBF	0.27 (0.026) b	36.6 (3.3) c
BBH	0.37 (0.024) a	36.9 (3.6) c
BBM	0.36 (0.025) a	55.6 (2.8) b
FBF	0.10 (0.006) c	37.6 (1.0) c
GBI	0.13 (0.013) c	11.9 (1.0) d
SDR	0.06 (0.005) d	68.6 (6.4) a

^a Values in parentheses indicate standard deviation. Same small case letter in vertical columns indicates no difference at 5% significance level.

significantly higher extrusion forces than the other materials. The extrusion forces of BBH and BBM were approximately six times higher than that of SDR, and three to four times higher than those of FBF and GBI.

For thread formation, the mean value ranged from 11.9 to 68.6 mm. GBI exhibited a significantly lower value than the other LVBRCs. SDR presented with significantly higher thread formation than the other materials, more than six times as high as GBI.

SEM Observations

Representative SEM images of the highly polished LVBRC specimens after argon ion etching are presented in Figure 1. Although each LVBRC showed differences in filler shape, size, and distribution, BBF, BBH, BBM, and SDR exhibited similar morphological features. They exhibited a wide range in size with irregular filler particles—from 0.1 to 10 μ m (Figures 1A, 1B, 1C, and 1F). Conversely, GBI employed densely packed nanosized irregular filler particles (Figure 1E). FBF consisted of nanosized spherical particles with aggregates of filler particles ranging from 0.5 to 3 μ m in size (Figure 1D).

Representative CLSM images of the wear facets and SEM images at the center of the facets are presented in Figure 2. The depth and width of the wear facet were material dependent. The wear facets in the BBF, BBM, and SDR specimens (Figures 2A, 2C, and 2F) were deeper and wider than those in the BBH, FBF, and GBI specimens. SEM revealed plucking of the large irregular filler particles in BBF, BBM, and SDR (indicated by white arrows), whereas BBH and GBI exhibited a similar wear pattern with a somewhat smooth surface (Figures 2B and 2E). While some cracks were observed (indicated by yellow arrows), detecting the plucking of fillers in the GBI specimens (Figures 2E) was difficult. The

surface of FBF was smooth, with some evidence of the plucking of the nanofillers (Figures 2D).

Correlation between the Tested Parameters in the LVBRCs

The Pearson product-moment correlation coefficients (r) and p values for the correlations between the tested parameters in the LVBRCs are presented in Table 8. Extremely strong negative and positive correlations were observed for the DOC versus EF, σ_F versus E , MD versus VL, and MD versus TF. All the correlations were statistically significant ($p < 0.05$), except for MD versus TF ($p = 0.067$). Strong negative correlations were observed for FC versus DOC, FC versus R , σ_F versus MD, σ_F versus VL, σ_F versus TF, E versus MD, E versus VL, E versus TF, R versus MD, R versus VL, and R versus EF, statistical significance notwithstanding ($p > 0.05$). Likewise, strong positive correlations were observed between FC and MD, FC and VL, FC and EF, and VL and TF, although they were not statistically significant ($p > 0.05$).

DISCUSSION

LVBRCs are thought to be suitable for base materials in deep cavities or for the restoration of narrow and deep cavities in nonstress-bearing areas.^{14,15} In recent years, the wear resistance of this resin composite has been improved to broaden the range of applicability.¹⁶ However, the available information on the use of LVBRCs in stress-bearing areas while maintaining the good handling properties and DOC is scarce.

The first and second null hypotheses were rejected, based on the results of this study. Although the LVBRCs showed different mechanical and handling properties depending on the type, some tested parameters showed strong correlations. Further, some LVBRCs showed excellent flexural strength and wear resistance while maintaining handling properties and DOC. In this study, the average DOC ranged from 3.10 to 4.36 mm. Although this value is influenced by light curing conditions, it has been shown that achieving an acceptable value (at 4 mm) is dependent on the material used.¹⁵ The three main strategies used to increase the curing depths of resin composites include the development of a more translucent resin composite, reduction in filler concentrations, and adoption of more efficient photoactivation systems.¹⁰⁻¹³ Matching the refractive indices of fillers and the resin matrix is considered as the best way to increase the DOC.¹⁰ Therefore, most of the LVBRCs are highly transparent when com-

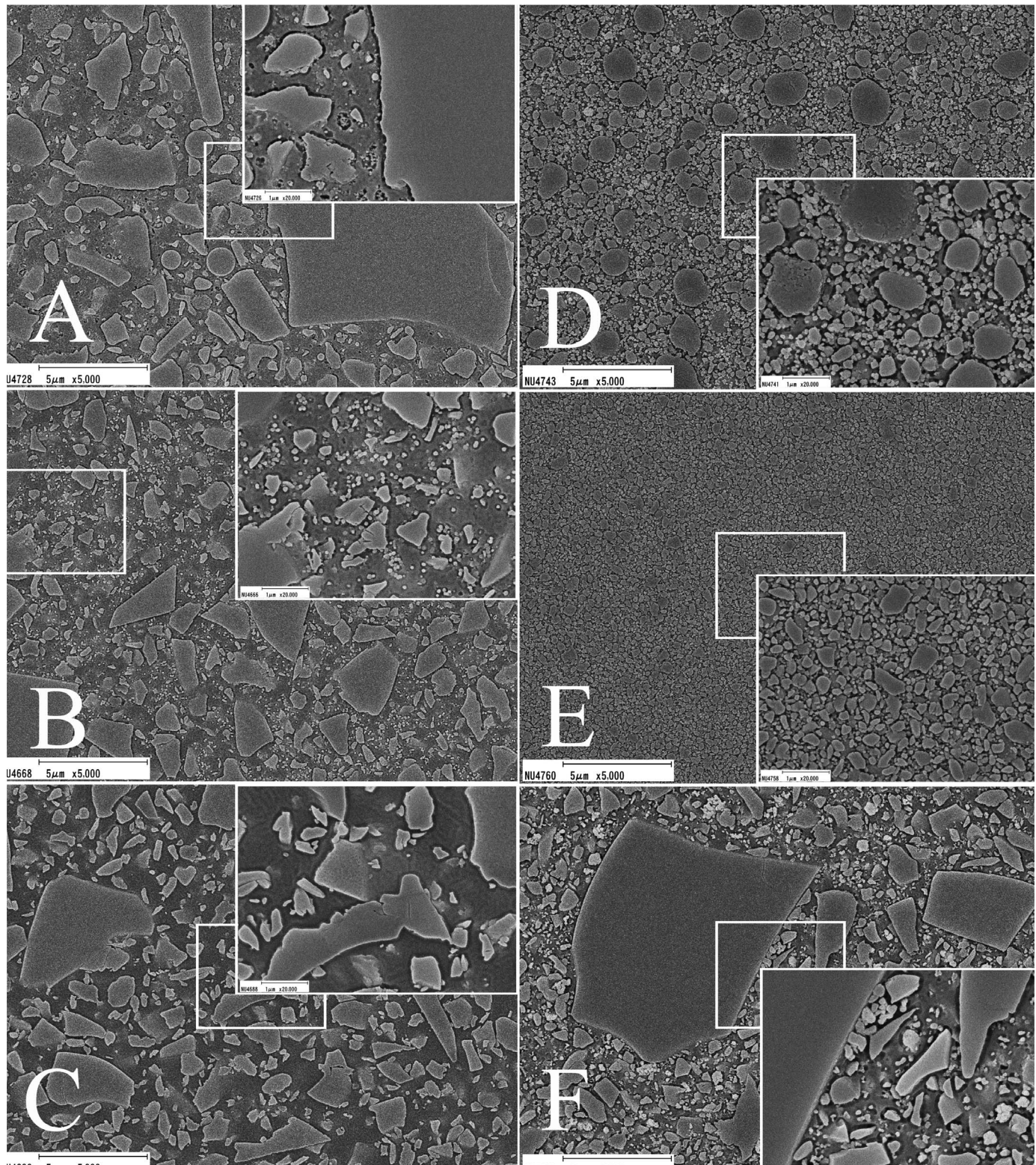


Figure 1. Scanning electron microscope (SEM) images of the argon-ion-etched surfaces of the low-viscosity bulk-fill resin composites (LVBRs). SEM images at magnifications 5000 \times and 20,000 \times .

- A. BBF
- B. BBH
- C. BBM
- D. FBF
- E. GBI
- F. SDR

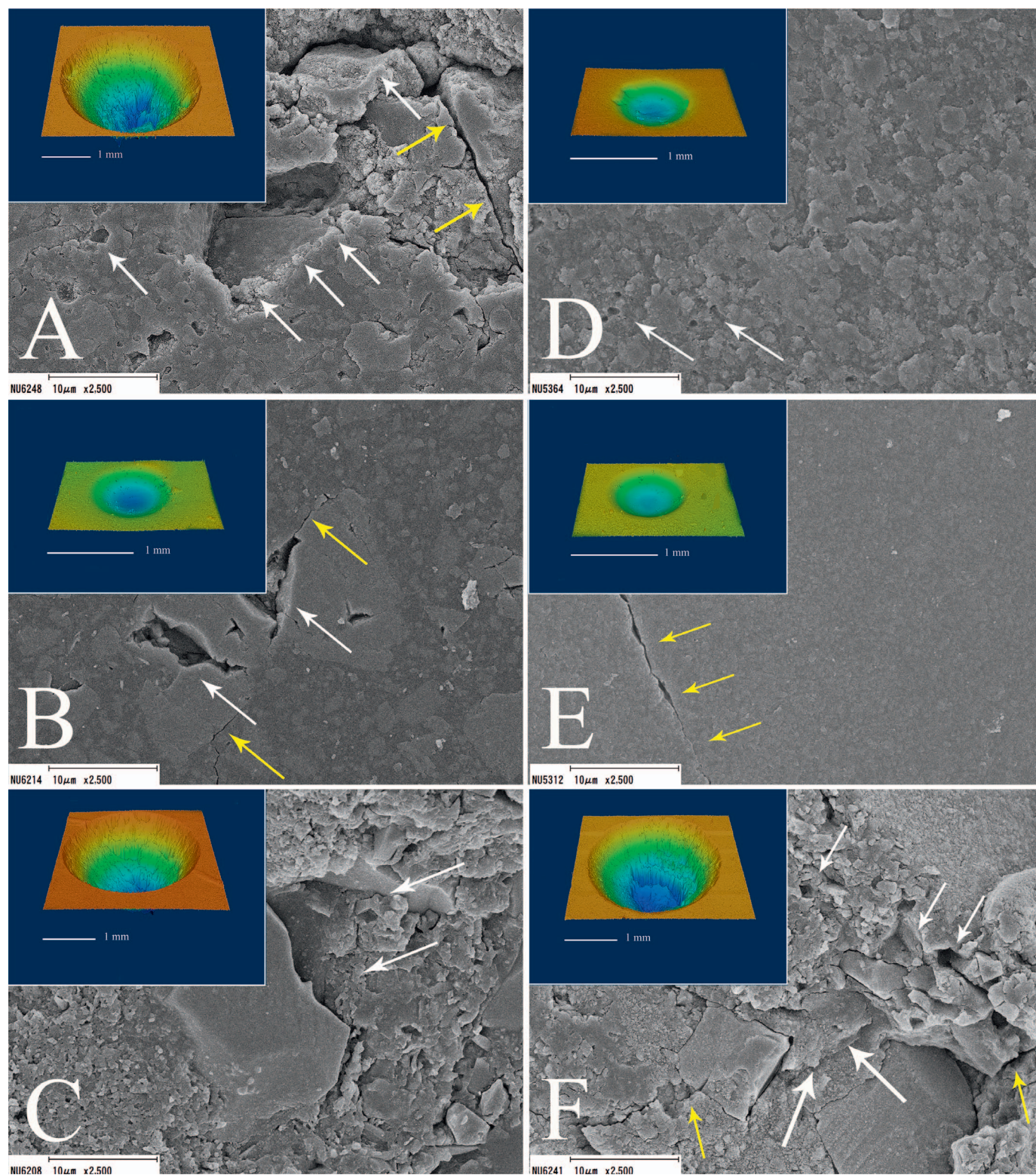


Figure 2. Representative wear facets of low-viscosity bulk-fill resin composites (LVBRCs) after the sliding impact wear test. Confocal laser scanning microscopy images of wear facet and scanning electron microscope (SEM) image of the center of the facet (2500 \times).

- A. BBF
- B. BBH
- C. BBM
- D. FBF
- E. GBI
- F. SDR

White arrows indicate evidence of the plucking of inorganic filler particles.
Yellow arrows indicate cracks.

Table 8: Correlation Between the Tested Parameters in the LVBRCs									
		DOC	σ_F	E	R	MD	VL	EF	TF
FC	r	−0.661	0.114	0.265	−0.554	0.504	0.514	0.540	0.221
	P value	0.153	0.830	0.612	0.254	0.308	0.297	0.268	0.674
DOC	r	0.006	−0.054	0.196	−0.096	−0.113	−0.923	−0.061	
	P value		0.991	0.918	0.709	0.856	0.831	0.009	0.908
σ_F	r		0.963	0.192	−0.696	−0.694	−0.124	−0.663	
	P value		0.006	0.716	0.125	0.126	0.815	0.151	
E	r			−0.140	−0.527	−0.501	0.013	−0.529	
	P value			0.792	0.283	0.311	0.981	0.280	
R	r				−0.561	−0.660	−0.417	−0.224	
	P value				0.246	0.154	0.411	0.670	
MD	r				0.986	0.101	0.779		
	P value				0.0003	0.849	0.067		
VL	r					0.171	0.692		
	P value					0.746	0.128		
EF	r						−0.011		
	P value						0.983		
Abbreviations: FC, Inorganic filler content; DOC, depth of cure; σ_F , Flexural strength; E, Elastic modulus; R, Resilience; MD, Maximum depth; VL, Volume loss; EF, Extrusion force; TF, Thread formation; r, correlation coefficient.									

pared with conventional flowable and universal resin composites. Although the present study confirmed a strong negative correlation between FC and the DOC, the reduction in filler content leads to reduced mechanical properties. Hence, the two strategies make it difficult to restore a cavity using only LVBRC in stress-bearing and esthetic areas. The filler details are different; for example, irregular fillers are believed to reduce light transmission owing to their higher levels of reflection.²⁰

Among the tested materials in this study, most resin composites exhibit a DOC of approximately 4 mm, except for BBH and BBM. The different DOCs in the different materials may be attributed to their composition. FBF had the lowest filler content, and consisted of nanosized spherical fillers and aggregated fillers (Figure 1D). Conversely, although SDR consisted of irregular fillers, the filler size was larger than those of the other materials (Figure 1F). Therefore, it can be hypothesized that filler properties play a significant role in light transmission and the DOC.^{10,21,22}

BBH and GBI exhibited significantly higher σ_F values than the other materials at both baseline and after TC. Conversely, BBM demonstrated a significantly lower σ_F value compared with the other LVBRCs. Although BBH and BBM were obtained from the same manufacturer, the instructions indicated that BBH can be used either as a veneer or base material, whereas BBM can only be used as a base (or lining) material. These two resins consisted

of the same resin monomers and filler types. Although the filler size, shape, and distribution were similar in BBH and BBM, several nanosized filler particles were observed between somewhat larger irregularly shaped fillers in BBH (Figures 1B and 1C). A possible explanation for the significant increase in σ_F value in BBH when compared with that in BBM is the presence of nanofillers that might inhibit crack propagation from external stress. However, the mixing ratios of the resin monomers might be different. GBI presented with a high σ_F value (>140 MPa), which was equal or superior to those of conventional flowable resin composites measured in a previous study.² The high σ_F value in the GBI specimen might be attributed to the densely packed, nanosized, irregular filler particles (Figure 1E) and the surface treatment of the inorganic fillers.

A statistically significant reduction in σ_F after TC when compared with the baseline was observed with all the materials. However, different reduction rates were observed among the materials (ranging from −4.8% to −14.3%). BBF and FBF exhibited higher reduction percentages than the other materials. The degradation process during TC is thought to be caused by thermal stress and water absorption.^{23,15} Although water susceptibility may be different in different resin monomers, the hydrophilic ether linkage in TEGDMA (*triethylene glycol dimethacrylate*), hydroxyl groups in *bis*-GMA (2, 2-bis[4-(2-hydroxy-3-methacryloyloxypropoxy)phenyl] pro-

pane), and urethane linkage in UDMA (*urethane dimethacrylate*) act as scaffolds for hydrolytic degradation.²⁴ A previous study reported the water sorption in three homopolymers in descending order as follows: TEGDMA > *bis*-GMA > UDMA.²⁴ Among the resin composites used in the current study, BBF and FBF employ *bis*-GMA and TEGDMA. Therefore, these resin monomer components might influence resin matrix degradation.

As for the σ_F , BBH demonstrated a significantly higher E value, and BBM presented with a significantly lower E value than the other LVBRCs. In general, resin composites tend to have increased E and σ_F values.²⁵ In the present study, an extremely strong positive correlation between σ_F and E was observed. Izabela and others²⁶ determined the E of three typical homopolymers and revealed that UDMA had a lower E than *bis*-GMA and TEGDMA, indicating that the resin monomer components may also affect the E of a resin composite. Most LVBRCs showed significantly higher E values in the TC group than in the baseline group. This may be due to the increase in the brittleness of the material as a result of the curing during TC.²⁷ Although resin composites with low E are more flexible and deform elastically under external stress, those with high E are stiff with a limited capacity to absorb the occlusal forces. Therefore, functional stresses might be transferred to the cavity walls if the E values of the materials increase over time.²⁸

R is considered as the material's ability to absorb energy when deformed elastically under external stress without failing.²⁷ Most LVBRCs demonstrated similar R values at baseline, and a statistically significant reduction in the R values was noted after TC in all the materials tested in this study. The temperature rise due to TC might increase the rigidity of the material due to postcure strengthening, and water immersion might change the material's properties due to plasticization by water absorption.²⁷

Based on the results of the wear test, the LVBRCs were classified into two groups: high- and low-wear resistance. Ujiie and others¹⁶ compared the wear resistance of flowable resin composites and LVBRCs using the Leinfelder–Suzuki (Alabama) localized wear test and reported that although LVBRCs exhibited a wide range of wear properties, some demonstrated similar wear behaviors to those of flowable resin composites. Although the wear method and apparatus used were different, the materials tested in that study included the three materials that were examined in the present study; addition-

ally, the outcome of the aforementioned study was in line with that of the current study. In both the studies, GBI exhibited the highest wear resistance when compared with the other LVBRCs. GBI employs densely packed ultrafine 150-nm barium fillers, and the interparticle space is obviously smaller than those in the other LVBRCs (Figure 1E). It is thought that the filler size influences the friction coefficient and surface roughness, which are the determining factors for the wear resistance of resin-based materials.²⁸ Smaller filler particles are related to lower friction coefficients and lead to lower internal shear stress in the resin matrix.²⁸ A lower wear rate was observed in FBF, which might be explained by a wear mechanism similar to that of GBI. Although FBF contains some large aggregated fillers consisting of nanosized zirconia/silica fillers, the interparticle spaces are filled with dispersed nanosized zirconia/silica fillers and small ytterbium trifluoride fillers. A previous investigation of the wear behavior of flowable resin composites using the same method as that in this study reported wear ranging from 49.4 to 110.7 μm for MD and 0.021 to 0.109 mm^3 for VL²; the levels of wear resistance of GBI, BBH, and FBF in the present study were similar to those of the flowable resin composites reported in their study. Therefore, in the results of mechanical properties and wear resistance, GBI and BBH can probably be used in stress-bearing areas while maintaining the DOC.

Conversely, BBF, BBM, and SDR exhibited approximately 15–20 times higher volumes of the VL for GBI, BBH, and FBF. BBF, BBM, and SDR have somewhat larger irregular particles and large interparticle space, resulting in lower wear resistance. In this study, the flexural properties (σ_F , E , and R) and wear properties (MD and VL) exhibited strong negative correlations, indicating that the low-wear resistance group showed low flexural properties. Hence, they are designed for use as base or lining materials owing to their lower mechanical properties.

In clinical situations, the force required to extrude the resin paste from a syringe is directly related to the ease of use. When the resin paste needs a stronger force to be extruded, it is more difficult to control the speed of the syringe plunger and the position of the tip. If the extrusion force is less, an excessive amount of resin paste might be pushed out from the syringe plunger. Moreover, if the resin paste forms threads, it might be difficult to control the amount of paste used and to create optimal anatomical forms when the syringe is withdrawn.

Table 9: The Definition of Abbreviations in This Study
LVBRC: Low-viscosity bulk-fill resin composite
BBF: Beautifil-Bulk
BBH: Bulk Base Hard
BBM: Bulk Base Medium
FBF: Bulk-Fill Flowable Restorative
GBI: G-ænial Bulk Injectable
SDR: SDR flow+
σ_F : Flexural strength
E : Elastic modulus
R : Resilience
TC: Thermal cycles
BRC: Bulk-fill resin composites
FC: Inorganic filler content
DOC: Depth of cure
MD: Maximum depth
VL: Volume loss
CLSM: Confocal laser scanning microscope
EF: Extrusion force
TF: Thread formation
r : Correlation coefficient
SEM: Scanning electron microscope
bis-GMA: 2, 2-bis[4-(2-hydroxy-3-methacryloyloxypropoxy)phenyl] propane
UDMA: Urethane dimethacrylate
TEGDMA: Triethylene glycol dimethacrylate
bis-MPEPP: 2, 2'-bis (4-methacryloxy polyethoxyphenyl) propane

The mean extrusion force values ranged from 0.10 to 0.37 MPa in the present study, and might have been affected by the types of resin monomers and their combinations. Aromatic dimethacrylates, such as *bis*-GMA and *bis*-MPEPP (2, 2'-bis(4-methacryloxy polyethoxyphenyl) propane), are frequently used as base monomers for resin-based materials.²⁹ These resin monomers include a hard segment containing a bisphenol backbone.²⁹ Although the viscosity of *bis*-MPEPP is considerably lower than those of *bis*-GMA and UDMA, it is higher than that of TEGDMA.^{30,31} BBH and BBM use the relatively low-viscosity *bis*-MPEPP, but do not contain TEGDMA, which may have resulted in the higher extrusion forces in these materials.

The mean value of thread formation was material dependent. Although the extrusion force of SDR was significantly lower than those of the other materials, it had a significantly higher thread formation, more than six times as high as GBI. Features such as the type of resin monomer, mixing ratio, and content, size, shape, and surface treatment of the filler may have influenced this phenomenon. However, regard-

ing the handling properties of LVBRCs in clinical situations, there is no doubt that a low extrusion force with less thread formation is preferable.

CONCLUSION

The present study revealed that the DOC, flexural properties, and wear resistance of LVBRCs are material dependent. The LVBRCs were classified into high- and low-wear resistance groups based on the wear behavior. BBH, FBF, and GBI exhibited higher wear properties than the other LBRCs and similar to those of recent flowable resin composites. The LVBRCs also showed a wide range of extrusion force and thread formation. The handling properties of this study can be helpful to select the preferable materials with objective indices. Extremely strong negative and positive correlations were observed for the DOC versus extrusion force, flexural strength versus elastic modulus, maximum depth versus volume loss, and maximum depth versus thread formation. Strong correlations between filler content and DOC, resilience, wear resistance, and extrusion force were observed. Likewise, the correlations between the DOC and extrusion force, flexural properties parameters and wear resistance, flexural properties parameters and thread formation, and wear parameters and thread formation were robust.

Acknowledgement

This work was supported in part by Grants-in-Aid for Scientific Research (grant nos. 19K10158) from the Japan Society for the Promotion of Science. This project was also supported in part by the Sato Fund and Uemura Fund, and by a grant from the Dental Research Center of the Nihon University School of Dentistry, Japan.

Conflict of Interest

The authors of this manuscript certify that they have no proprietary, financial, or other personal interest of any nature or kind in any product, service, and/or company that is presented in this article.

(Accepted 23 January 2021)

References

1. Ferracane JL (2011) Resin composite-state of the art *Dental Materials* **27**(1) 29-38. <https://doi.org/10.1016/j.dental.2010.10.020>

2. Imai A, Takamizawa T, Sugimura R, Tsujimoto A, Ishii R, Kawazu M, Saito T, & Miyazaki M (2019) Interrelation among the handling, mechanical, and wear properties of the newly developed flowable resin composites *Journal of the Mechanical Behavior of Biomedical Materials* **89**(1) 72-80. <https://doi.org/10.1016/j.jmbbm.2018.09.019>

3. Bayne SC, Thompson JY, Swift EJ Jr, Stamatiades P, & Wilkerson M (1988) A characterization of first-generation

- flowable composites *Journal of the American Dental Association* **129**(5) 567-77. <https://doi:10.14219/jada.archive.1998.0274>
4. Irie M, Tjandrawinata R, Lihua E, Yamashiro T, & Suzuki K (2008) Flexural performance of flowable versus conventional light-cured composite resins in a long-term in vitro study *Dental Materials Journal* **27**(2) 300-309. <https://doi:10.4012/dmj.27.300>
 5. Sumino N, Tsubota K, Takamizawa T, Shiratsuchi K, Miyazaki M, & Latta MA (2013) Comparison of the wear and flexural characteristics of flowable resin composites for posterior lesions *Acta Odontologica Scandinavica* **71**(3-4) 820-827.
 6. Lazaridou D, Belli R, Petschelt A, & Lohbauer U (2015) Are resin composites suitable replacements for amalgam? A study of two-body wear *Clinical Oral Investigations* **19**(6) 1485-1492.
 7. Rosatto CMP, Bicalho AA, Veríssimo C, Bragança GF, Rodrigues MP, Tantbirojn D, Versluis A, & Soares CJ (2015) Mechanical properties, shrinkage stress, cuspal strain and fracture resistance of molars restored with bulk-fill composites and incremental filling technique *Journal of Dentistry* **43**(12) 1519-1528. <https://doi:10.1016/j.jdent.2015.09.007>
 8. Veloso SRM, Lemos CAA, de Moraes SLD, do Egito Vasconcelos BC, Pellizzer EP, & de Melo Monteiro GQ (2019) Clinical performance of bulk-fill and conventional resin composite restorations in posterior teeth: a systematic review and meta-analysis *Clinical Oral Investigations* **23**(1) 221-233. <https://doi:10.1007/s00784-018-2429-7>
 9. Boaro LCC, Lopes DP, de Souza ASC, Nakano EL, Perez MDA, Pfeifer CS, & Gonçalves F (2019) Clinical performance and chemical-physical properties of bulk fill composites resin—a systematic review and meta-analysis *Dental Materials* **35**(10) e249-e264. <https://doi:10.1016/j.dental.2019.07.007>
 10. Bucuta S & Ilie N (2014) Light transmittance and micro-mechanical properties of bulk fill vs. conventional resin based composites *Clinical Oral Investigation* **18**(8) 1991-2000. <https://doi:10.1007/s00784-013-1177-y>
 11. Kim EH, Jung KH, Son SA, Hur B, Kwon YH, & Park JK (2015) Effect of resin thickness on the microhardness and optical properties of bulk-fill resin composites *Restorative Dentistry & Endodontics* **40**(2) 128-135. <https://doi:10.5395/rde.2015.40.2.128>
 12. Engelhardt F, Hahnel S, Preis V, & Rosentritt M (2016) Comparison of flowable bulk-fill and flowable resin-based composites: An in vitro analysis *Clinical Oral Investigation* **20**(8) 2123-2130. <https://doi:10.1007/s00784-015-1700-4>
 13. Al Sunbul H, Silikas N, & Watts DC (2016) Polymerization shrinkage kinetics and shrinkage-stress in dental resin-composites *Dental Materials* **32**(8) 998-1006. <https://doi:10.1016/j.dental.2016.05.006>
 14. Van Ende A, De Munck J, Lise DP, & Van Meerbeek B (2017) Bulk-fill composites: A review of the current literature *Journal of Adhesive Dentistry* **19**(2) 95-109. <https://doi:10.3290/j.jad.a38141>
 15. Lima RBW, Troconis CCM, Moreno MBP, Murillo-Gómez F, & De Goes MF (2018) Depth of cure of bulk fill resin composites: A systematic review *Journal of Esthetic and Restorative Dentistry* **30**(6) 492-501. <https://doi:10.1111/jerd.12394>
 16. Ujiie M, Tsujimoto A, Barkmeier WW, Jurado CA, Villalobos-Tinoco J, Takamizawa T, Latta MA, & Miyazaki M (2020) Comparison of occlusal wear between bulk-fill and conventional flowable resin composites *American Journal of Dentistry* **33**(2) 74-78.
 17. Price RBT, Ferracane JL, & Shortall AC (2015) Light-curing units: a review of what we need to know *Journal of Dental Research* **94**(9) 1179-1186. <https://doi:10.1177/0022034515594786>
 18. International Organization for Standardization (2009) ISO 4049:2009. Dentistry—Polymer-based restorative materials. International Organization for Standardization, Geneva, Switzerland.
 19. Peutzfeldt A & Asmussen E (1992) Modulus of resilience as predictor for clinical wear of restorative resins *Dental Materials* **8**(3) 146-148. [https://doi:10.1016/0109-5641\(92\)90071-j](https://doi:10.1016/0109-5641(92)90071-j)
 20. Arikawa H, Kanie T, Fujii K, Takahashi H, & Ban S (2007) Effect of filler properties in composite resins on light transmittance characteristics and color *Dental Materials Journal* **26**(1) 38-44. <https://doi:10.4012/dmj.26.38>
 21. Emami N, Sjudahl M, & Soderholm KJ (2005) How filler properties, filler fraction, sample thickness and light source affect light attenuation in particulate filled resin composites *Dental Materials* **21**(8) 721-730. <https://doi:10.1016/j.dental.2005.01.002>
 22. Fujita K, Ikemi T, & Nishiyama N (2011) Effects of particle size of silica filler on polymerization conversion in a light-curing resin composite *Dental Materials* **27**(11) 1079-1085. <https://doi:10.1016/j.dental.2011.07.010>
 23. De Munck J, Van Landuyt KL, Peumans M, Poitevin A, Lambrechts P, Braem M, & Van Meerbeek B (2005) A critical review of the durability of adhesion to tooth tissue: methods and results *Journal of Dental Research* **84**(4) 118-132. <https://doi:10.1177/154405910508400204>
 24. Venz S & Dickens B (1991) NIR-spectroscopic investigation of water sorption characteristics of dental resins and composites *Journal of Biomedical Materials Research* **25**(10) 1231-1248. <https://doi:10.1002/jbm.820251005>
 25. Shibasaki S, Takamizawa T, Nojiri K, Imai A, Tsujimoto A, Endo H, Suzuki S, Suda S, Barkmeier WW, Latta MA, & Miyazaki M (2017) Polymerization behaviour and mechanical properties of high-viscosity bulk fill and low shrinkage resin composites *Operative Dentistry* **42**(6) e177-e187. <https://doi:10.2341/16-385-L>
 26. Izabela M & Barszczewska R (2009) Structure-property relationships in dimethacrylate networks based on Bis-GMA, UDMA and TEGDMA *Dental Materials* **25**(9) 1082-1089. <https://doi:10.1016/j.dental.2009.01.106>
 27. Akiba S, Takamizawa T, Tsujimoto A, Moritake N, Ishii R, Barkmeier WW, Latta MA, & Miyazaki M (2019) Influence of different curing modes on flexural strength, fracture toughness, and wear behavior of dual-cure

- provisional resin-based composites *Dental Materials Journal* **38**(5) 728-737. <https://doi:10.4012/dmj.2018-300>
28. Heintze SD, Reichl FX, & Hickel R (2019) Wear of dental materials: Clinical significance and laboratory wear simulation methods - a review *Dental Materials Journal* **38**(3) 343-353. <https://doi:10.4012/dmj.2018-140>
29. Kawaguchi M, Fukushima T, & Horibe T (1987) Mechanical and physical properties of 2, 2'-bis (4-methacryloxy polyethoxyphenyl) propane polymers *Dental Materials Journal* **6**(2) 148-155. <https://doi:10.4012/dmj.6.148>
30. Silikas N & Watts DC (1999) Rheology of urethane dimethacrylate and diluent formulations *Dental Materials* **15**(4) 257-261. [https://doi:10.1016/s0109-5641\(99\)00043-3](https://doi:10.1016/s0109-5641(99)00043-3)
31. Tanoue N, Mikami A, Atsuta M, & Matsumura H (2007) Effects of monomer composition and original filler loading in the resulting centrifuged composites *Dental Materials Journal* **26**(4) 501-505. <https://doi:10.4012/dmj.26.501>